15.4   A 107pJ/b 100kb/s 0.18μm Capacitive-Coupling Transceiver for Printable Communication Sheet

Lechang Liu[1], Makoto Takamiya[1], Tsuyoshi Sekitani[1],
Yoshiaki Noguchi[1], Shintaro Nakano[1], Koichiro Zaitsu[1],
Tadahiro Kuroda[2], Takao Someya[1], Takayasu Sakurai[1]

[1]University of Tokyo, Tokyo, Japan, [2]Keio University, Yokohama, Japan

Low-power wireless communications between electronic objects scattered over tables, walls and ceiling will form an infrastructure necessary for wireless sensor networks and ambient intelligence. A data edge-signaling scheme and DC power-free pulse detector allow the realization of a low energy/bit transceiver for use in a communication sheet [1], as shown in Fig. 15.4.1(a), which allows the creation of infrastructure for ambient electronics when used together with the wireless power transmission sheet [2].

An overview of the whole communication system is shown in Fig. 15.4.1(b). By combining meter-scale wired communication and μm-scale wireless capacitive coupling communication, the sheet offers a communication method that enables multiple electronic objects scattered over the sheet to communicate contactlessly with each other, by establishing communication paths without cumbersome physical connections. In this application differential signaling is required, because there is no common ground among the TX sheet, the communication sheet and RX sheet. Since the information transmitted over the sheet is confined in a small space close to ad hoc routed paths, the system is free from issues related with radio frequency band allocation. The communication route is dynamically formed using plastic MEMS switches, and an organic nonvolatile memory stores the routing information [1]. As illustrated in Fig. 15.4.1(c), the communication sheet is composed of 8×8 units and every unit consists of four pads. The communication between two units is achieved by turning on the adjacent two MEMS switches and the top two routing switches. Thus, only four switches are required for point-to-point communication.

The device structure of the communication sheet is shown in Fig. 15.4.2. It consists of five low-cost printed sheets [1]: a 16×16 9.7mm² pad array for capacitive coupling, two 9×8 MEMS-switching matrices for differential signal routing, a 9×8 organic nonvolatile memory array for routing information storage and a 8×8 position-sensing coil array [2]. The communication between the pad of the TX/RX and the pad on the sheet is similar to conventional chip-to-chip communication. In the sheet communication system, however, the available maximum effective inductance is about 10μH and the worst case parasitic capacitance is 50pF, which are different from chip-to-chip communication. If the received signal is large enough so that the power consumption of receiver can be ignored, the power-consumption of the whole system is only determined by the transmitter. The energy-consumption of capacitive coupling and inductive coupling can be approximated by CV^2 and LI^2, respectively. For the given parameters, the energy-consumption of capacitive coupling is lower than inductive coupling at less than 3.5MHz. In this application the typical data rate is 100kb/s and therefore capacitive coupling instead of inductive coupling [1] is used.

For capacitive coupling, a key constraint to consider is that when a long string of "1's" and "0's" is passed through a high-pass filter, the signal experiences the "zero wander" effect. Conventionally, feedback control is introduced to generate a complementary signal to compensate the decaying signal [3]. The input NRZ (Non-Return-Zero) signal is converted into a return-to-V_{DD}/2 signal pulse to avoid this constraint. Figure 15.4.3 shows the schematics of the proposed transmitter and receiver. The modulated data is achieved by switching the input data and the output of the half-V_{DD} generator [4]. The driver stage of the half-V_{DD} generator has zero power dissipation with half-V_{DD} signals. The edge detector is used to generate the switching signal for the selector by detecting both the rising and falling edge of the input data. Compared to previous synchronous circuits [5], asynchronous circuits have no global clocks and the operation is triggered by signal transitions, potentially having the advantages of low power dissipation. To detect a small signal, an

amplifier and a comparator is often used in the first stage of the receiver to amplify the received signal for the next demodulation. The major disadvantage of this topology is large DC power dissipation that occurs even for no AC input. In the transmitted signal of the communication sheet, the circuit spends long periods of time with no AC signal. Power dissipated in these periods is wasted. A pulse detector can alleviate this problem by having essentially zero power dissipation for no AC input. Two unbalanced inverters are used to detect the rising edge and falling edge, respectively, and the detection results are level-shifted to V_{DD}. As shown in Fig. 15.4.3, if the gate input of the pulse detector is a positive pulse and the bias input is a negative pulse, the corresponding data edge can be detected. To tune the sensitivity of proposed pulse detector, a variable bias voltage (V_{DD}/2-ΔV) for the source input of the pulse detector is used.

A test chip was designed and fabricated in 0.18μm 1P6M CMOS and the micrograph is shown in Fig. 15.4.4(a). The measured performance is summarized in Fig. 15.4.4(b). The developed data edge signaling and the DC power-free pulse detector enable 107pJ/b energy-consumption at 100kb/s. Figure 15.4.5 shows the measured waveforms at 100kb/s and the eye diagram at the maximum data rate of 8Mb/s. Figure 15.4.6(a) shows the simulated dependence of the RX power consumption on the data transition probability at 100kb/s. For the 50% data transition probability, the power consumption of the receiver can be reduced by 30%, which shows the advantage of the proposed data edge signaling scheme over the previous synchronous signaling scheme [5]. To increase the sensitivity of the receiver, the bias voltage (V_{DD}/2-ΔV) of the pulse detector in Fig. 15.4.3 should be reduced but the power consumption will be increased. Figure 15.4.6(b) shows the measured ΔV dependence of the RX power consumption and the minimum detectable RX voltage. The tradeoff between the power and the RX sensitivity is tuned by ΔV. The high RX sensitivity is required to compensate the voltage reduction due to horizontal displacement of the RX pads and the distance between RX pads and the pads of the communication sheet. The measured minimum ΔV for different displacement and distance of the pads to achieve the 100kb/s communication is illustrated in Fig. 15.4.6(c). For the normal 75μm distance, which is equal to the sheet thickness and corresponds to 52pF coupling capacitance, the sheet can operate with up to 3.75mm displacement. The maximum tolerable displacement was 7.5mm, which corresponds to the 77% of the pad size. Figure 15.4.7 shows a comparison with the state-of-art communication systems. The power-consumption of the communication sheet is lower than conventional wireless communication systems. Thus the communication method presented, which combines the mobility of wireless communication and the low-power performance of wireline communication simultaneously, bridges the gap between wire-line and wireless communication.

References:
[1] T. Sekitani, et al., "Communication Sheets using Printed Organic Nonvolatile Memories," *IEDM*, Paper 9.3, Dec. 2007.
[2] M. Takamiya, et al., "Design Solutions for Multi-Object Wireless Power Transmission Sheet Based on Plastic Switches," *ISSCC Dig. Tech. Papers*, pp. 362-363, Feb. 2007.
[3] T. J. Gabara and W. C. Fischer, "Capacitive Coupling and Quantized Feedback applied to Conventional CMOS Technology," *IEEE J. Solid-State Circuits*, vol. 32, pp. 419-427, Mar. 1997.
[4] S. Fujii, et al., "A 50μA Standby 1MW × 1b/256KW × 4b CMOS DRAM," *ISSCC Dig. Tech. Papers*, pp. 266-268, Feb. 1986.
[5] K. Kanda, D. D. Antono, K. Ishida, and T. Sakurai, "1.27Gb/s/pin 3mW/pin Wireless Super-Connect (WSC) Interface Scheme," *ISSCC Dig. Tech. Papers*, pp. 288-289, Feb. 2003.
[6] R. Palmer, et al., "A 14mW 6.25Gb/s Transceiver in 90nm CMOS for Serial Chip-to-Chip Communications," *ISSCC Dig. Tech. Papers*, pp. 440-441, Feb. 2007.
[7] I. D. O'Donnell, and R. Brodersen, "A 2.3mW Baseband Impulse-UWB Transceiver Front-End in CMOS," *IEEE Symp. on VLSI Circuits*, pp. 200-201, June, 2006.
[8] J. R. Bergervoet, et al., "A WiMedia-Compliant UWB Transceiver in 65nm CMOS," *ISSCC Dig. Tech. Papers*, pp. 112-113, Feb. 2007.
[9] M. Simon, et al., "An 802.11a/b/g RF transceiver in an SoC," *ISSCC Dig. Tech. Papers*, pp. 562-563, Feb. 2007.
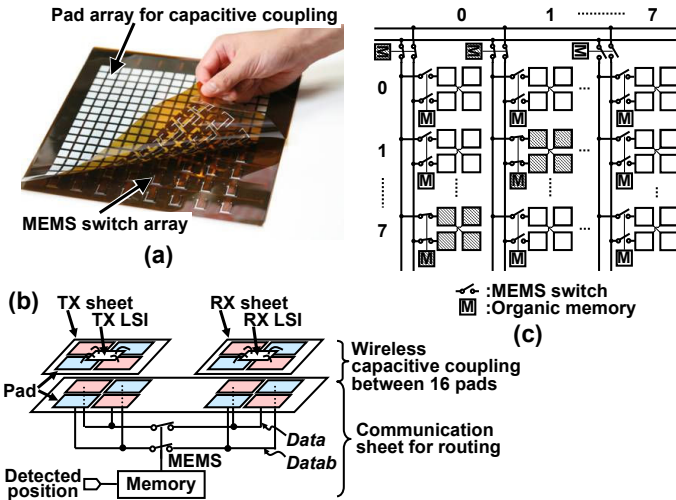
Figure 15.4.1: Communication sheet. (a) Bird's-eye photo. (b) Principle of operation. (c) Circuit schematic.
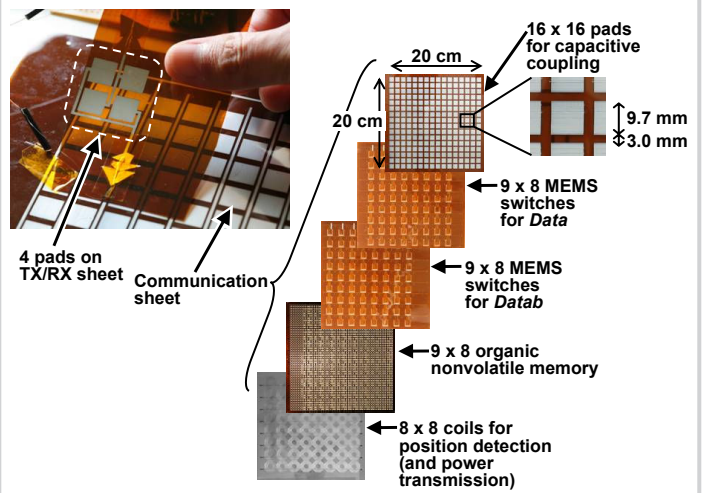
Figure 15.4.2: Device structure of communication sheet.
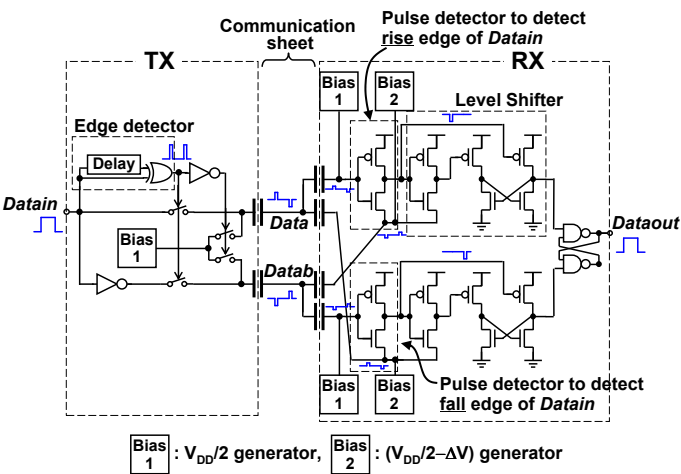
Figure 15.4.3: Schematic of transceiver with data edge signaling and DC power-free pulse detector.

Technology		0.18μm CMOS
Supply Voltage		1.8V
Data Rate	Typ	100kb/s
	Max	8Mb/s
Communi-cation Distance	Capacitive Coupling	150μm
	Wireline	60cm
Alignment Tolerance		7.5mm
Power @100kb/s	TX	9.73μW
	RX	0.97μW
	Total	10.7μW
Energy per bit		107pJ/b
Core Area	TX	2475μm²
	RX	975μm²

(b)
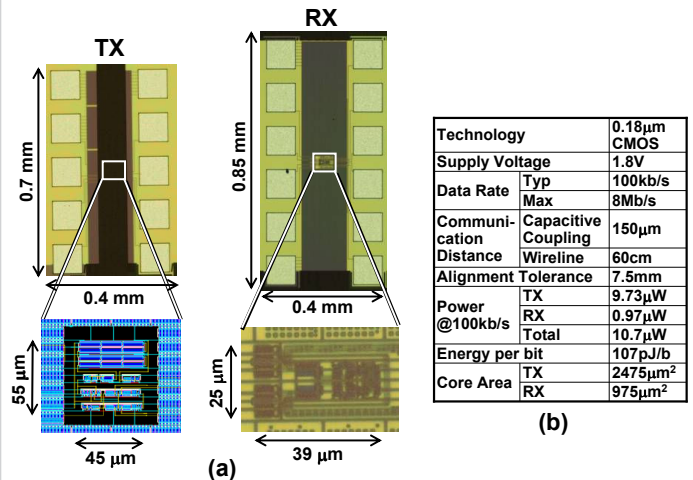
Figure 15.4.4: (a) Chip micrographs and layout of TX and RX. (b) Performance summary.
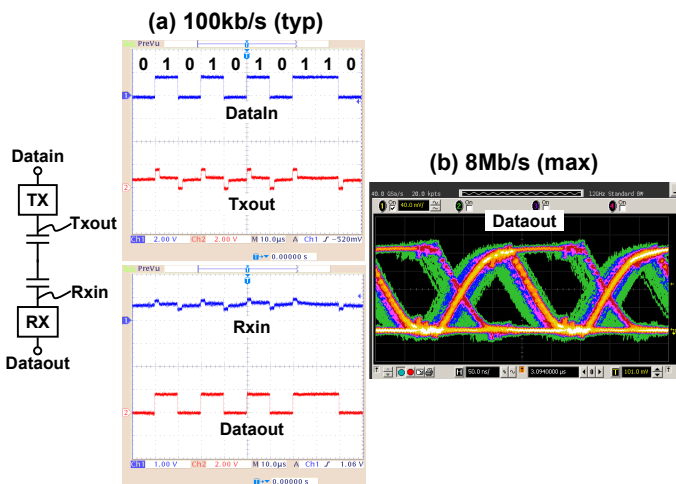
Figure 15.4.5: (a) Measured waveforms at 100kb/s. (b) Eye diagram at maximum data rate of 8Mb/s.
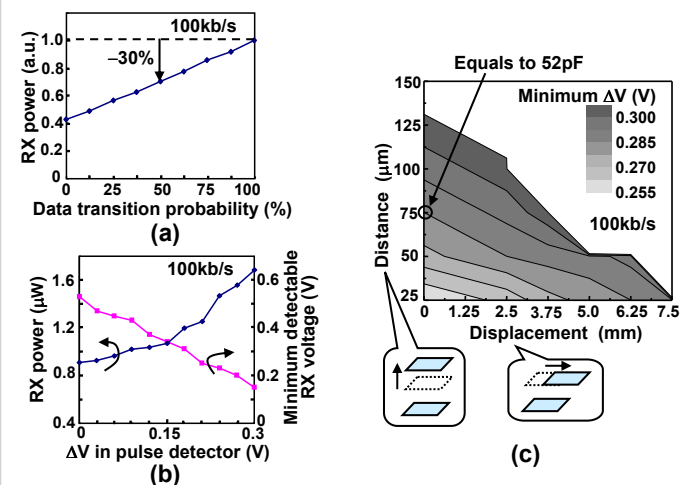
Figure 15.4.6: (a) Simulated dependence of the RX power consumption on data transition probability. (b) Measured ΔV dependence of RX power consumption and minimum detectable RX voltage. (c) Measured minimum ΔV for different displacement and distance of the pads.

15
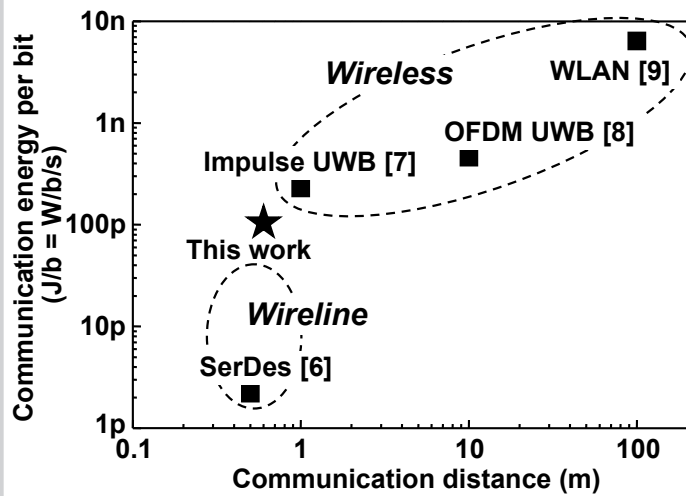
Figure 15.4.7: Comparison with the state-of-art wireless and wireline communications.